

Deep Ad-Hoc Beamforming

Xiao-Lei Zhang

Abstract—Although deep learning based speech enhancement methods have demonstrated good performance in adverse acoustic environments, their performance is strongly affected by the distance between the speech source and the microphones since speech signals fade quickly during the propagation. To address the above problem, we propose *deep ad-hoc beamforming*—a deep-learning-based multichannel speech enhancement method with an ad-hoc microphone array. It serves for scenarios where the microphones are placed randomly in a room and work collaboratively. It aims to pick up speech signals with equally high quality in a range where the array covers. Its core idea is to reweight the estimated speech signals with a sparsity constraint when conducting adaptive beamforming, where the weights produced by a neural network are an estimation of the propagation cost from the speech source to the ad-hoc microphone array, e.g. signal-to-noise ratios, and the sparsity constraint is to filter out the microphones that are too far away from both the speech source and the majority of the ad-hoc microphone array. We conducted an extensive experiment in a scenario where the location of the speech source is far-field, random, and blind to the microphones. Results show that our method outperforms representative deep-learning-based speech enhancement methods by a large margin.

Index Terms—Adaptive beamforming, ad-hoc microphone array, channel reweighting, channel selection, deep learning, distributed microphone array, MVDR.

I. INTRODUCTION

DEEP learning based speech enhancement has demonstrated its strong denoising ability in adverse acoustic environments [1], which has attracted much attention since its first appearance [2]. Current deep-learning-based techniques employ either a single microphone or a conventional microphone array to pick up speech signals. Deep-learning-based single-channel speech enhancement, e.g. [2], [3], employs a deep neural network (DNN), which is a multilayer perceptron with more than one nonlinear hidden layer, to learn a nonlinear mapping function from noisy speech to clean speech or its ideal time-frequency masks. Deep-learning-based multichannel speech enhancement can be categorized to two branches. The first branch uses a microphone array as a feature extractor to extract spatial features, e.g. interaural time difference and interaural level difference, as the input of the DNN-based single-channel enhancement [4]. The second branch, which we denote bravely as *deep beamforming*, estimates a monaural time-frequency (T-F) mask [5] using a single-channel DNN

This work was supported in part by the National Natural Science Foundation of China (NSFC) funding scheme under Project No. 61671381, in part by the Project of the Science, Technology, and Innovation Commission of Shenzhen Municipality under grant No. JCYJ20170815161820095, and in part by the Shaanxi Natural Science Basic Research Program under grant No. 2018JM6035.

Xiao-Lei Zhang is with the Center for Intelligent Acoustics and Immersive Communications, School of Marine Science and Technology, Northwestern Polytechnical University, Xi'an, China (e-mail: xiaolei.zhang@nwpu.edu.cn).

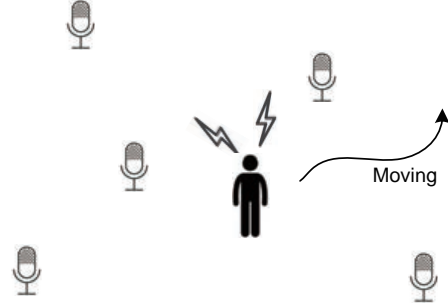


Fig. 1. Illustration of an ad-hoc microphone array.

so that the spatial covariance matrices of speech and noise can be derived for adaptive beamforming [6], [7], e.g. minimum variance distortionless response (MVDR) or generalized eigenvalue beamforming.

Although DNN-based single-channel speech enhancement methods improve speech quality and intelligibility, the enhanced speech suffer from nonlinear distortions. It is observed frequently that, when applying a single-channel enhancement front-end to a speech recognition system, the recognition rate is even lower than that on the original noisy speech. Therefore, people have to train the front-end and the speech recognition system jointly, which is not only complicated in engineering but also sensitive to the variations of the microphone receivers.

Deep beamforming is a solution to the above problem. It is fundamentally linear methods, whose output does not suffer from nonlinear distortions. Deep beamforming and its application to robust speech recognition has been extensively studied [6]–[17] since its first appearance [6], [7], including the aspects of acoustic features [13], [18], model training [14]–[17], mask estimations [8], post-processing [19], etc. Although many positive results have been observed, existing deep beamforming techniques were studied with conventional microphone arrays only, such as linear arrays in portable equipments. Because speech signals fade quickly during the propagation through air, the performance of deep beamforming drops significantly when the distance between the speech source and the microphone array is enlarged. Finally, how to maintain the enhanced speech at the same high quality throughout an interested physical space becomes a new problem.

Ad-hoc microphone arrays provide a potential solution to the above problem. As illustrated in Fig. 1, an ad-hoc microphone array is a set of randomly distributed microphones. The microphones collaborate with each other. Compared to conventional microphone arrays, an ad-hoc microphone array has the following two potentials. First, it has a chance to enhance a speaker's voice with equally good quality in a

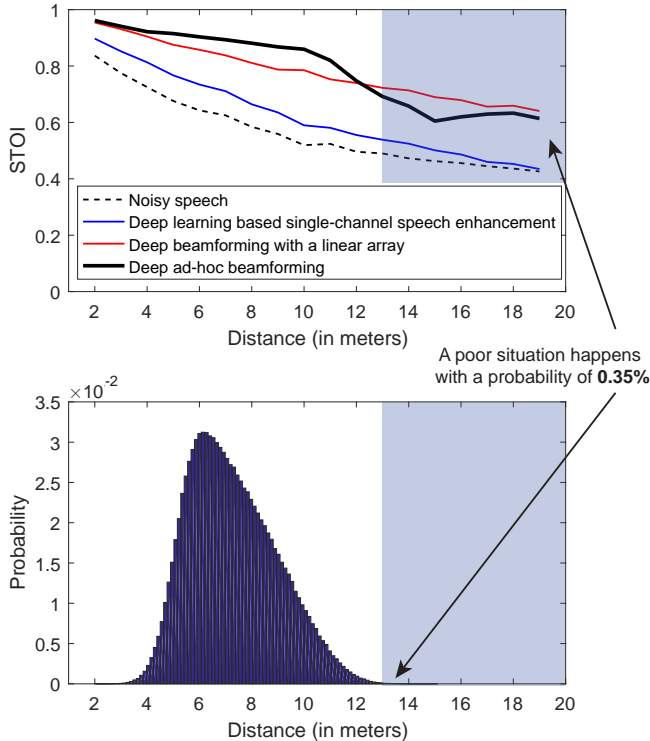


Fig. 2. An example of the experimental result of this paper. (a) STOI results of the comparison methods in a room where the distance between a speech source and a microphone is limited to the range of $[1, 20]$ meters. The environment is diffuse babble noise. The distance between the speech source and the ad-hoc microphone array is the average distance between the speech source and all microphones in the array. Deep beamforming uses a linear microphone array with a size of 0.4 meter. Both the linear array and the ad-hoc array contain 16 microphones. (b) A Monte Carlo simulation of the probability density function of the distance distribution between the speech source and the ad-hoc microphone array. The simulation result shows that, when both the speech source and the array are placed randomly in the room, the situation where deep ad-hoc beamforming performs poorer than deep beamforming happens with a probability of only 0.35%.

range where the array covers. Second, its performance is not limited to the physical size of application devices, e.g. cell-phones, gooseneck microphones, or smart speaker boxes. Ad-hoc microphone arrays also have a chance to be widespread in real-world environments, such as meeting rooms, smart homes, and smart cities. The research on ad-hoc microphone arrays is an emerging direction [20]–[28]. However, current research on ad-hoc microphone arrays is still at the very beginning. For example, some work has focused on the channel selection problem in an ideal scenario where perfect noise estimation and voice activity detection is available [21], [27]. Although some work has tried to jointly conduct noise estimation and channel selection, it has to make many assumptions and carry out advanced mathematical formulations [22], [24].

In this paper, we propose *deep ad-hoc beamforming* (DAB), to our knowledge, the first DNN-based multichannel speech enhancement method for ad-hoc microphone arrays. DAB is a supervised method. It revises the signal model of the DNN-based minimum variance distortionless response (MVDR) beamforming [6], [7] by reweighting the channels according to the quality of the received signals at the microphones, where the weights of the channels are produced from a channel-

reweighting model trained by supervised off-line learning. The channel-reweighting model contains two modules. The first module uses a neural network to estimate the propagation cost from the speech source to the ad-hoc microphone array, e.g. signal-to-noise ratios. The second module uses sparsity constraints to filter out the microphones that are too far away from both the speech source and the majority of the ad-hoc microphone array.

We have conducted an extensive experimental comparison between the representative deep-learning based single-channel enhancement, deep beamforming, and DAB when the speech sources and microphone arrays were placed randomly in typical physical spaces. Experimental results with both noise-dependent training and noise-independent training show that DAB outperforms the comparison methods by a considerable margin with a small performance variance throughout the spaces. For example, suppose a microphone array contains 16 microphones, then a representative of the experimental result can be viewed in Fig. 2 where DAB reaches an average short-time intelligibility measure (STOI) score of 88.02% with a variance of 1.96%, while the single-channel method reaches an average STOI score of 68.84% with a variance of 9.88%, and deep beamforming reaches an average STOI score of 82.50% with a variance of 6.30%.

This paper is organized as follows. Section III formulates the problem. Section IV presents the proposed DAB. Sections V and VI present the experimental results with noise-dependent and noise-independent models respectively. Finally, Section VII concludes our findings.

II. NOTATIONS

We first introduce some notations here. Regular small letters, e.g. s , f , and γ , indicate scalars. Bold small letters, e.g. \mathbf{y} and $\boldsymbol{\alpha}$, indicate vectors. Bold capital letters, e.g. \mathbf{P} and Φ , indicate matrices. Letters in calligraphic fonts, e.g. \mathcal{X} , indicate sets. $\mathbf{0}$ ($\mathbf{1}$) is a vector with all entries being 1 (0). The operator T denotes the transpose. The operator H denotes the conjugate transpose of complex numbers. The operator \odot denotes the elementwise product. The abbreviation “s.t.” is short for “subject to”.

III. MOTIVATION AND PROBLEM FORMULATION

A. Deep beamforming

All speech enhancement methods throughout the paper operate in the frequency domain on a frame-by-frame basis. Suppose that a physical space contains one target speaker, multiple noise sources, and a conventional microphone array (e.g. a linear array) of M microphones. The physical model for the received signals by the microphone array is assumed to be

$$\mathbf{y}(t, f) = \mathbf{c}(f)s(t, f) + \mathbf{n}(t, f) \quad (1)$$

where $s(t, f)$ is the short-time Fourier transform (STFT) value of the target clean speech at time t and frequency f , $\mathbf{c}(f)$ is assumed to be a time-invariant acoustic transfer function from

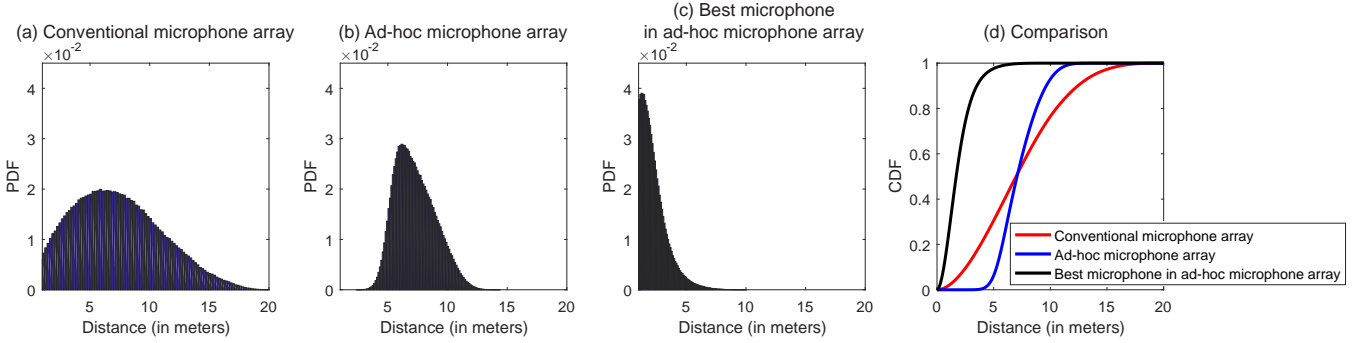


Fig. 3. Monte Carlo simulation of the distance distribution between a speech source and a microphone array in comparison. The physical spaces for this simulation contain a square room, a rectangle room, and a circle room. The farthest distance between the speech source and the microphone array in any of the rooms is limited to 20 meters. Each microphone array in comparison consists of 16 microphones. (a) Probability density function (PDF) of the distance distribution of a conventional microphone array. The mean and standard deviation of this distribution are 7.28 and 3.71 meters respectively. (b) PDF of the distance distribution of an ad-hoc microphone array, where the distance is defined as the average distance between the speaker and each microphone in the ad-hoc array. The mean and standard deviation of this distribution are 7.28 and 1.68 meters respectively. (c) PDF of the distribution of the distance between the speech source and the best microphone in the ad-hoc microphone array, where the word “best microphone” denotes the closest microphone to the speech source. The mean and standard deviation of the distribution are 1.92 and 1.21 meters respectively. (d) Cumulative distribution functions (CDF) of the distance distributions in Figs. 3a, 3b, and 3c.

the speaker to the array which is an M -dimensional complex number:

$$\mathbf{c}(f) = [c_1(f), c_2(f), \dots, c_M(f)]^T \quad (2)$$

and $\mathbf{y}(t, f)$ and $\mathbf{n}(t, f)$ are the received noisy speech and noise respectively:

$$\mathbf{y}(t, f) = [y_1(t, f), y_2(t, f), \dots, y_M(t, f)]^T \quad (3)$$

$$\mathbf{n}(t, f) = [n_1(t, f), n_2(t, f), \dots, n_M(t, f)]^T. \quad (4)$$

with $y_m(t, f)$ and $n_m(t, f)$ as the STFT values of the received signals by the m -th microphone at time t and frequency f .

An adaptive beamformer finds a linear estimator $\mathbf{w}_{\text{opt}}(f)$ to filter $\mathbf{y}(t, f)$ by the following equation:

$$\hat{\mathbf{s}}(t, f) = \mathbf{w}_{\text{opt}}^H(f) \mathbf{y}(t, f). \quad (5)$$

where $\hat{\mathbf{s}}(t, f)$ is an estimate of $\mathbf{s}(t, f)$. For example, MVDR finds \mathbf{w}_{opt} by minimizing the average output power of the beamformer while maintaining the energy along the target direction, which is formulated as the following quadratic programming problem:

$$\begin{aligned} \mathbf{w}_{\text{opt}}(f) &= \arg \min_{\mathbf{w}(f)} \mathbf{w}^H(f) \mathbf{\Phi}_{\mathbf{nn}}^{-1}(f) \mathbf{w}(f) \\ \text{s.t.} \quad & \mathbf{w}^H(f) \mathbf{c}(f) = 1 \end{aligned} \quad (6)$$

where $\mathbf{\Phi}_{\mathbf{nn}}(f)$ is an $M \times M$ -dimensional cross-channel covariance matrix of the received noise signal $\mathbf{n}(f)$. (6) has a closed-form solution, where the variables $\mathbf{\Phi}_{\mathbf{nn}}(f)$ and $\mathbf{c}(f)$ need to be derived first from a noise estimation algorithm, i.e. an estimate of $\mathbf{n}(f)$. The noise estimation is not only crucial for the success of the adaptive beamforming, but also the main challenge of the research.

Deep beamforming, e.g. [6], [7], uses a single-channel time-frequency masking technique [5] to estimate $\mathbf{n}(f)$ accurately. Moreover, unlike traditional statistical signal processing methods, the process of estimating $\mathbf{n}(f)$ does not need to know the pattern of the array, which makes it flexible to many kinds of microphone arrays, such as linear array, circular array, etc.

B. Ad-hoc microphone arrays

A fundamental factor affecting the performance of a speech enhancement method is the distance between the speech source and the microphone receiver. For example, as shown in Fig. 2, if the microphone of a deep-learning-based single-channel method could be placed about two meters closer to the speech source, then we are able to reach the same STOI level as before even though we do not conduct any speech enhancement.

Given the above phenomenon, we should pay more attention to make microphones have a high probability to be close to the speaker, instead of simply focusing on improving the performance of a speech enhancement method given fixed noisy speech. Ad-hoc microphone arrays provide such an opportunity. As shown in Fig. 3, when a speaker and a microphone array are distributed randomly in a room, an ad-hoc microphone array has a smaller variance than a conventional microphone array (Figs. 3a and 3b), so that it is supposed to reach more stable performance than the latter. Moreover, the best microphone in the ad-hoc microphone array is close to the speaker (Fig. 3c), no matter where the speaker appears in the room.

Due to the above advantages, we propose to apply deep-learning-based speech enhancement to ad-hoc microphone arrays, i.e. DAB. Two questions arise: (i) should we pick up the signals from all microphones with equally important weights as deep beamforming, since deep beamforming does not need to know the pattern of the array? No, we cannot do so, due to the fact that the distances between the speaker and the microphones in an ad-hoc microphone array vary in a large range as shown in Fig. 1, and the quality of the received signals may vary dramatically accordingly as shown in Fig. 4. From [6], [7], we know that, if the DNN-based time-frequency (T-F) masking is not accurate enough which is a situation that the ad-hoc microphone array meets, then $\mathbf{w}_{\text{opt}}(f)$ can be problematic. (ii) Can we just pick up the signal from the “best” microphone that is the closest one to the speaker as the final output of DAB directly, given the distance distribution of

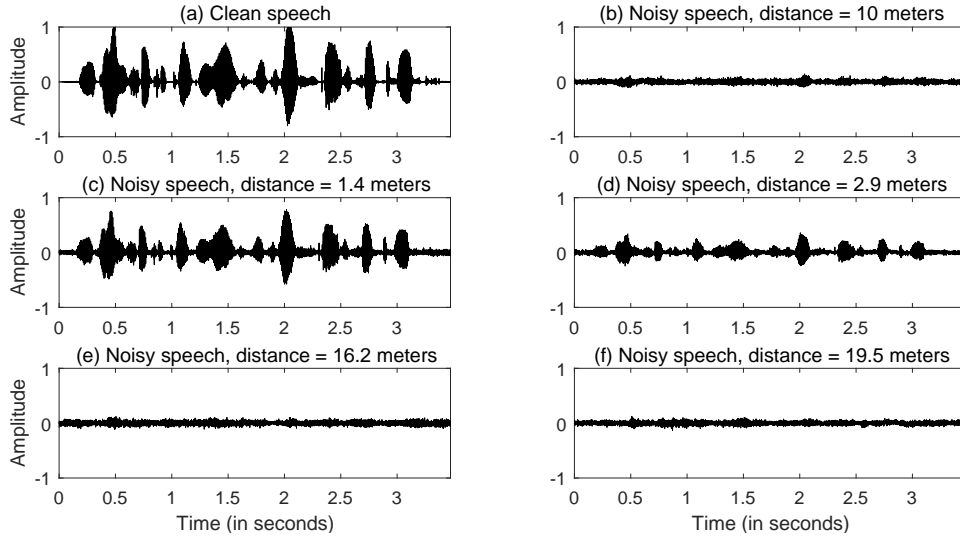


Fig. 4. An example of the noisy speech signals collected by a conventional microphone array and an ad-hoc microphone array, where both arrays consist of 4 microphones and are 10 meters away from the speech source. (a) Ground-truth clean speech. (b) Noisy speech collected by a microphone in the conventional array. (c)-(f) Noisy speech collected by the ad-hoc microphone array where the 4 microphones are placed at the locations of 1.4, 2.9, 16.2, and 19.5 meters from the speech source.

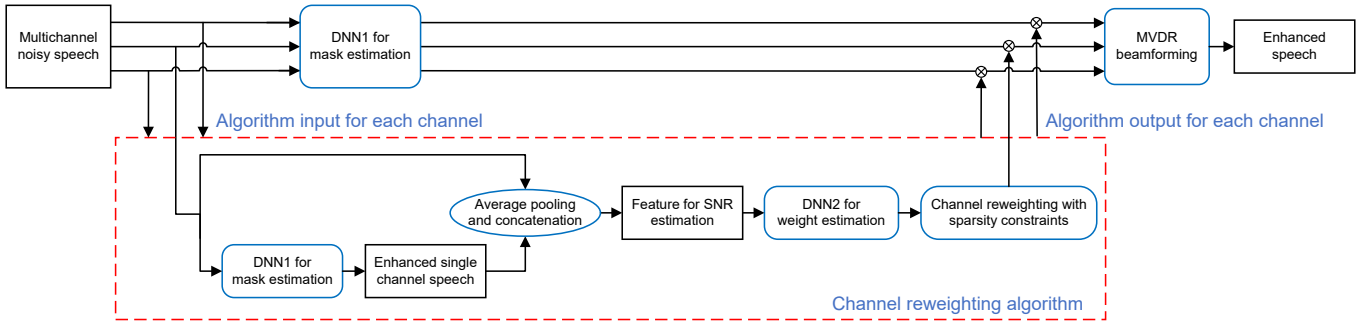


Fig. 5. Diagram of deep ad-hoc beamforming. The channel-reweighting algorithm is described in the red dashed box.

the microphone in Fig. 3c? This is probably not the optimal way. As shown in Fig. 4 and later in the experiments, the signals from other microphones nearby are also informative.

A compromise to the aforementioned two questions is to reweight the channels with sparsity based on their transmission costs, such as signal-to-noise ratios (SNR). To summarize, the signal model for ad-hoc microphone arrays should be rectified.

IV. DEEP AD-HOC BEAMFORMING

The core idea of DAB is to filter $\mathbf{y}(t, f)$ by a channel-reweighting vector $\mathbf{p} = [p_1, \dots, p_M]^T$ before the adaptive beamforming, such that the channels that output low quality speech signals can be suppressed or even discarded. A system overview is shown in Fig. 5.

In this section, we first overview the DAB system in Section IV-A, then describe the module of single-channel time-frequency masking (i.e. DNN1 in Fig. 5) in Section IV-B, and at last propose a channel-reweighting algorithm (i.e. the algorithm in the red dashed box in Fig. 5) in Section IV-C.

A. System overview

1) *Signal model*: If we denote $\mathbf{x}(t, f) = \mathbf{c}(f)s(t, f)$, then (1) can be rewritten as

$$\mathbf{y}(t, f) = \mathbf{x}(t, f) + \mathbf{n}(t, f). \quad (7)$$

The signal model considered in this paper is

$$\mathbf{y}_{\mathbf{p}}(t, f) = \mathbf{p} \odot \mathbf{y}(t, f) = \mathbf{p} \odot \mathbf{x}(t, f) + \mathbf{p} \odot \mathbf{n}(t, f) \quad (8)$$

where \mathbf{p} is the output of a channel-reweighting model $g(\cdot)$, see Section IV-C for the details about $g(\cdot)$. We denote the covariance matrices of $\mathbf{y}(t, f)$, $\mathbf{x}(t, f)$, and $\mathbf{n}(t, f)$ over time as $\Phi_{\mathbf{y}\mathbf{y}}(f)$, $\Phi_{\mathbf{x}\mathbf{x}}(f)$, and $\Phi_{\mathbf{n}\mathbf{n}}(f)$, respectively. Assuming that $\mathbf{x}(t, f)$ and $\mathbf{n}(t, f)$ are uncorrelated, then we have

$$\Phi_{\mathbf{y}\mathbf{y}}(f) = \Phi_{\mathbf{x}\mathbf{x}}(f) + \Phi_{\mathbf{n}\mathbf{n}}(f) \quad (9)$$

so as to

$$\mathbf{P} \odot \Phi_{\mathbf{y}\mathbf{y}}(f) = \mathbf{P} \odot \Phi_{\mathbf{x}\mathbf{x}}(f) + \mathbf{P} \odot \Phi_{\mathbf{n}\mathbf{n}}(f) \quad (10)$$

where $\mathbf{P} = \mathbf{p}\mathbf{p}^T$. We further denote

$$\Phi_{\mathbf{p}, \mathbf{v}\mathbf{v}}(f) = \mathbf{P} \odot \Phi_{\mathbf{y}\mathbf{y}}(f), \quad \forall \mathbf{v} \in \{\mathbf{y}, \mathbf{x}, \mathbf{n}\}. \quad (11)$$

2) *MVDR beamformer*: This paper takes MVDR beamformer as an implementation of DAB, though many other adaptive beamformers can be applied as well.

Using $\Phi_{\mathbf{p},\text{nn}}(f)$ to replace $\Phi_{\text{nn}}(f)$ in (6) derives $\mathbf{w}_{\text{opt}}(f)$ and $\hat{s}(t, f)$ as

$$\mathbf{w}_{\text{opt}}(f) = \frac{\hat{\Phi}_{\mathbf{p},\text{nn}}^{-1}(f)\hat{\mathbf{c}}(f)}{\hat{\mathbf{c}}^H(f)\hat{\Phi}_{\mathbf{p},\text{nn}}^{-1}(f)\hat{\mathbf{c}}(f)} \quad (12)$$

$$\hat{s}(t, f) = \mathbf{w}_{\text{opt}}^H(f)\mathbf{y}_{\mathbf{p}}(t, f) \quad (13)$$

where $\hat{\Phi}_{\mathbf{p},\text{nn}}(f)$ is an estimate of $\Phi_{\mathbf{p},\text{nn}}(f)$:

$$\hat{\Phi}_{\mathbf{p},\text{nn}}(f) = \frac{1}{\sum_t \eta(t, f)} \sum_t \eta(t, f)\mathbf{y}_{\mathbf{p}}(t, f)\mathbf{y}_{\mathbf{p}}^H(t, f) \quad (14)$$

and $\hat{\mathbf{c}}(f)$ is an estimate of $\mathbf{c}(f)$, which is the first principal component of an estimated covariance matrix $\hat{\Phi}_{\mathbf{p},\text{xx}}(f)$:

$$\hat{\Phi}_{\mathbf{p},\text{xx}}(f) = \frac{1}{\sum_t \xi(t, f)} \sum_t \xi(t, f)\mathbf{y}_{\mathbf{p}}(t, f)\mathbf{y}_{\mathbf{p}}^H(t, f) \quad (15)$$

with $\eta(t, f)$ and $\xi(t, f)$ defined as the product of individual estimated T-F masks:

$$\eta(t, f) = \prod_{i=1}^N (1 - \hat{m}_i(t, f)), \quad \xi(t, f) = \prod_{i=1}^N \hat{m}_i(t, f) \quad (16)$$

where $\hat{m}_i(t, f)$ is an estimate of the ideal T-F mask produced by a regression model $h(\cdot)$ (denoted as DNN1 in Fig. 5) at the i -th channel. See Section IV-B for the details about $h(\cdot)$. The derivation of the MVDR beamformer is similar to that in [13].

B. Single-channel time-frequency masking

Suppose the STFT feature is F -dimensional. We denote

$$\hat{\mathbf{m}}_i(t) = [\hat{m}_i(t, 1), \dots, \hat{m}_i(t, F)]^T \quad (17)$$

$$\tilde{\mathbf{y}}_i(t) = [|\tilde{y}_i(t, 1)|, \dots, |\tilde{y}_i(t, F)|]^T \quad (18)$$

where $|y|_i(t, f)$ is the amplitude spectrogram of $\mathbf{y}(t, f)$ at the i -th channel. $\hat{\mathbf{m}}_i(t)$ is produced by DNN1 via

$$\hat{\mathbf{m}}_i(t) = h(\tilde{\mathbf{y}}_i(t)). \quad (19)$$

In the training stage of $h(\cdot)$, we construct a corpus \mathcal{X}_1 containing the amplitude spectrograms of single-channel noisy speech and its corresponding noise and clean speech components, which are denoted as $|y|(t, f)$, $|s|(t, f)$, and $|n|(t, f)$ respectively. $h(\cdot)$ takes the ideal ratio mask (IRM) as the training target:

$$\text{IRM}(t, f) = \frac{|s|(t, f)}{|s|(t, f) + |n|(t, f)}, \quad \forall f = 1, \dots, F \quad (20)$$

See [5] for the details on how to train a single-channel DNN model for the prediction of the IRM.

TABLE I
TRAINING TARGETS OF THE CHANNEL-REWEIGHTING MODEL.

Name	Definition
Signal to noise ratio (DAB-SNR)	$\frac{\sum_t s _{\text{time}}(t)}{\sum_t n _{\text{time}}(t)}$
Signal to signal plus noise ratio (DAB-S2NR)	$\frac{\sum_t s _{\text{time}}(t)}{\sum_t s _{\text{time}}(t) + \sum_t n _{\text{time}}(t)}$

C. Channel-reweighting algorithm

1) *Channel-reweighting models*: Given a test utterance of U frames, we first merge all noisy frames and the estimated clean speech respectively to two vectors by average pooling:

$$\tilde{\mathbf{y}}_i = \frac{1}{U} \sum_{t=1}^U \tilde{\mathbf{y}}_i(t), \quad \tilde{\mathbf{s}}_i = \frac{1}{U} \sum_{t=1}^U \hat{\mathbf{s}}_i(t), \quad \forall i = 1, \dots, M \quad (21)$$

where $\hat{\mathbf{s}}_i(t) = \hat{\mathbf{m}}_i(t) \odot \tilde{\mathbf{y}}_i(t)$. Then, we concatenate $\tilde{\mathbf{y}}_i$ and $\tilde{\mathbf{s}}_i$ as the input of $g(\cdot)$:

$$q_i = g\left(\left[\tilde{\mathbf{y}}_i^T, \tilde{\mathbf{s}}_i^T\right]^T\right), \quad \forall i = 1, \dots, M. \quad (22)$$

We train $g(\cdot)$ by supervised learning. To train $g(\cdot)$, we need to first define a training target. Many factors affect the definition of a training target, such as the propagation cost of speech signals through air, battery life of a cell phone, etc. This paper considers two propagation costs related to SNR. Specifically, suppose that a noisy speech sequence in the time domain and its corresponding clean speech and noise components at a microphone are $\{y_{\text{time}}(t)\}_t$, $\{s_{\text{time}}(t)\}_t$, and $\{n_{\text{time}}(t)\}_t$, respectively. We define two training targets of $g(\cdot)$ in Table I. According to the definitions of the targets, it is easy to see that DAB-S2NR is limited to the range of $[0, 1]$, while the range of DAB-SNR is unlimited. We will focus on investigating DAB-S2NR throughout the experiments, leaving DAB-SNR as a reference.

We need to construct another training corpus \mathcal{X}_2 excluded from \mathcal{X}_1 to train $g(\cdot)$, so as to prevent overfitting. We first take the noisy speech in \mathcal{X}_2 as the input of DNN1, and then use the estimated clean speech produced by DNN1 as part of the training data $\hat{\mathbf{s}}$. Because $g(\cdot)$ deals with segment-level features, \mathcal{X}_2 should be much larger than \mathcal{X}_1 in practice. This paper uses a neural network as $g(\cdot)$ given its scalability, though many regression models can be used as well. The neural network model is denoted as DNN2 in Fig. 5.

2) *Channel-selection method*: Given the estimated weights $\mathbf{q} = [q_1, \dots, q_M]^T$ of a test utterance, we aim to learn a binary mask $\mathbf{b} = [b_1, \dots, b_M]^T$, such that the channel-reweighting vector \mathbf{p} is given by:

$$\mathbf{p} = \mathbf{q} \odot \mathbf{b}. \quad (23)$$

Substituting (23) to (8) finishes the prediction process of the channel-reweighting algorithm.

Claim 1. \mathbf{b} is calculated by the following equation:

$$b_i^{\text{(DAB-SNR)}} = \begin{cases} 1, & \text{if } \frac{q_i}{q_*} > \gamma \\ 0, & \text{otherwise} \end{cases}, \quad \forall i = 1, \dots, M. \quad (24)$$

$$b_i^{(\text{DAB-S2NR})} = \begin{cases} 1, & \text{if } \frac{q_i}{q_*} \frac{1-q_*}{1-q_i} > \gamma, \\ 0, & \text{otherwise} \end{cases}, \quad \forall i = 1, \dots, M. \quad (25)$$

where $q_* = \max_{i \in \{1, \dots, M\}} q_i$, the symbol $*$ $\in \{1, \dots, M\}$ is the identifier of q_* , and $\gamma \in [0, 1]$ is a tunable threshold.

Proof. We denote the energy of the clean and noise components of the test utterance at the i -th channel as S_i and N_i respectively, i.e. $S = \sum_t |s|_{\text{time}}(t)$ and $N = \sum_t |n|_{\text{time}}(t)$. Our core idea is to filter out the signals of the channels whose clean speech satisfies:

$$S_i < \gamma S_* \quad (26)$$

Under the assumptions that the estimated weights are perfect and that the statistics of the noise components are consistent across the channels, we have

$$q_i = \frac{S_i}{N_*}, \quad q_* = \frac{S_*}{N_*} \quad (27)$$

for DAB-SNR, and

$$q_i = \frac{S_i}{S_i + N_*}, \quad q_* = \frac{S_*}{S_* + N_*} \quad (28)$$

for DAB-S2NR. Substituting (27) into (26) derives (24); and substituting (28) into (26) derives (25). Claim 1 is proved. \square

We find in our experiments that $\gamma = 0.5$ yields generally good performance.

Note that many advanced sparse learning methods are able to be applied instead of our simple channel-selection method. Here we focus on presenting the importance of the channel-selection in DAB, leaving the problem of developing a highly-effective channel-selection algorithm as future work.

V. EXPERIMENTS WITH NOISE-DEPENDENT MODELS

The term *noise-dependent* means that the noise scenarios of the training and test sets of machine-learning-based models are the same in terms of noise types and SNR levels.

This section studies the properties of DAB with noise-dependent training. Specifically, we first present the experimental settings in Section V-A. Then, we present the main experimental results in Section V-B. At last, we analyze the channel-reweighting algorithm in Section V-C.

A. Experimental settings

1) *Room simulations:* We simulated three rooms as shown in Fig. 6 whose shapes are common in our real-world life. In each room, a speech source and a microphone (array) are placed randomly, and the farthest distance from the speech source to the microphone is limited to at most 20 meters. If not specified, the distance between a speech source and an ad-hoc microphone array is the average distance between the speech source and each microphone of the array. Fig. 3a summarizes the probability density function (PDF) of the distance distribution of a single microphone and a conventional microphone array in all three rooms. Fig. 3b summarizes the PDF of the distance distribution of an ad-hoc microphone array in all three rooms by Monte-Carlo simulation. From Figs. 3a,

3b, and 6, it is easy to see that the distance distribution of the ad-hoc microphone array has a smaller variance than the conventional microphone array.

The clean speech propagates at a speed of 343 meters per second. Its amplitude is fading at a rate of $1/r$ where r is the distance from the speech source. It is corrupted by additive noise. We assumed that (i) the space has weak or no reverberation, (ii) the additive noise is diffuse noise whose energy distributes evenly across the entire space, and (iii) the additive noise between two locations is uncorrelated.

2) *Datasets:* The clean speech was generated from the TIMIT corpus. TIMIT consists of a training set and a test set. The training set contains 462 speakers. The test set contains 168 speakers. Each speaker has 10 utterances. Each utterance is about 3 seconds long. We randomly selected half of the training speakers to construct the database for training DNN1, and the remaining half for training DNN2. We used all test speakers for test. The additive noise was the babble, factory1, and volvo noise from the NOISEX-92 database respectively. For each noise scenario, its noise audio recording was split to three segments, which were used to synthesize the noisy utterances for the DNN1 training, DNN2 training, and test, respectively. For both training and test, the SNR level at a place of 1 meter away from the speech source, denoted as *the SNR at the origin*, was set to 15 dB. The SNR level of each synthesized noisy utterance further decreases according to the distance between the origin and the microphone. The time delay of the clean speech component is determined by the sound speed and the distance between the origin and the microphone. We synthesized 30,000 noisy utterances to train DNN1. For each noisy utterance, we randomly select one clean utterance and mixed it with a random part of the noise segment at a random distance in the range of [1, 20] meters. Similarly, we synthesized 100,000 noisy utterances to train DNN2. We have conducted many tests, see Section V-A for their detailed descriptions. For each test, we produced 1680 clean utterances from the speech source, and recorded their noisy counterparts at any necessary location of a microphone for evaluation.

3) *Comparison methods:* We compared the proposed deep ad-hoc beamforming with a DNN-based nonlinear single-channel speech enhancement method and deep beamforming:

- **Deep-learning-based nonlinear single-channel speech enhancement (DS):** For each test utterance, the distance between the speech source and the microphone was randomly generated from [1 : 1 : 20] meters, where the symbol $[a : b : c]$ denotes a set of integer numbers starting from a and ending at c with an interval of b . DS takes the IRM as the target.
- **Deep beamforming (DB):** We adopted three linear microphone arrays with 4, 8, and 16 microphones respectively, each of which has a size of 0.4 meter. We conducted experiments on each microphone array. For each test utterance in each experiment, the distance between the speech source and the microphone array was randomly generated from [1 : 1 : 20] meters. The DB in comparison is similar to the method in [13, Section 2.1].
- **Deep ad-hoc beamforming (DAB):** We adopted three ad-hoc microphone arrays with 4, 8, and 16 microphones

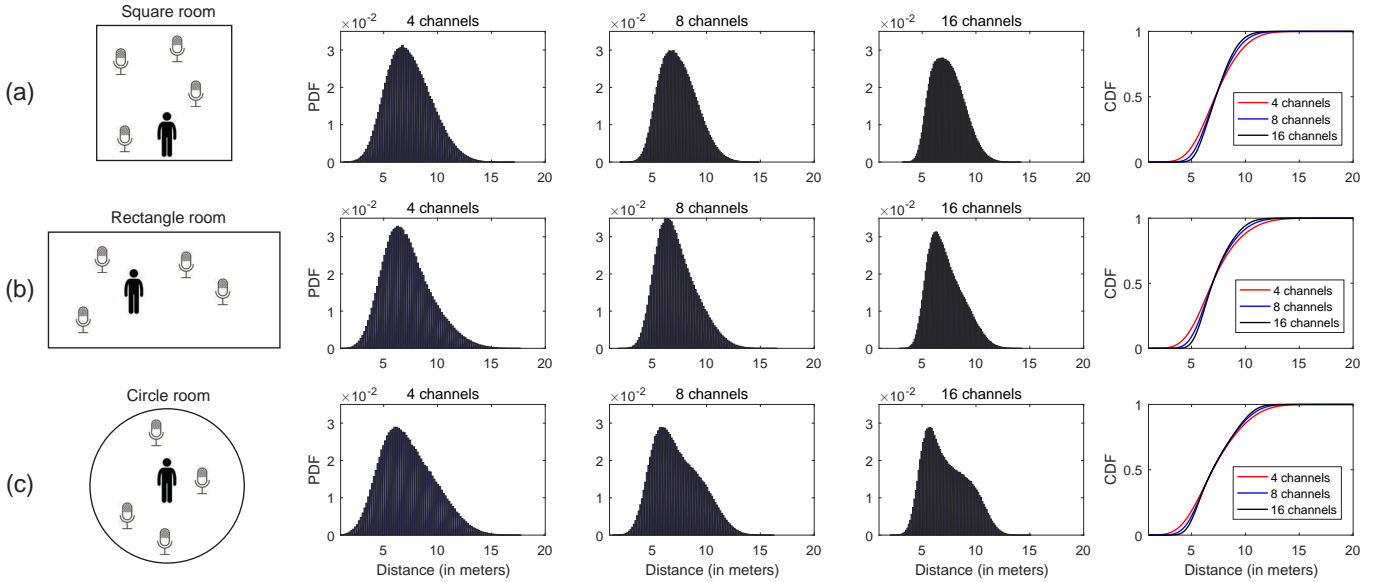


Fig. 6. Distributions of the distances between the randomly distributed speech sources and the ad-hoc microphone arrays with 4, 8, and 16 microphones respectively in (a) a square room with a size of 14.14×14.14 square meters, (b) a rectangle room with a size of 17.89×8.94 square meters, and (c) a circle room with a diameter of 20 meters.

respectively. We conducted experiments on each microphone array. For each test utterance in each experiment, we first randomly generated a distance from $[1 : 1 : 20]$ meters as the distance between the speech source and the microphone array, and then assigned each microphone in the array a distance randomly generated from $[1, 20]$ and satisfying the constraint that the average distance assigned to the microphones equals to the distance between the speech source and the microphone array.

We set the frame length and frame shift to 32 and 16 milliseconds respectively, and extracted 257-dimensional STFT features. We used the same DNN1 for DS, DB, and DAB. The parameter setting of DNN1 is as follows. DNN1 is a standard feedforward DNN. It contains two hidden layers. Each hidden layer has 1024 hidden units. The activation functions of the hidden units and output units are rectified linear unit and sigmoid function, respectively. The number of epochs was set to 50. The batch size was set to 512. The scaling factor for the adaptive stochastic gradient descent was set to 0.0015, and the learning rate decreased linearly from 0.08 to 0.001. The momentum of the first 5 epochs was set to 0.5, and the momentum of other epochs was set to 0.9. A contextual window was used to expand each input frame to its context along the time axis. The window size was set to 5.

The parameter setting of DNN2 for DAB was as follows. It contains one hidden layer with 1024 hidden units. The number of epochs was set to 50. The batch size was set to 32. The target DAB-S2NR was used in all experiments, while DAB-SNR was only studied as a reference in Section V-C1. All other parameters were set to the same values as DNN1. When DAB-SNR was studied, it was normalized globally to the range $[0, 1]$ so as to fit the output range of the sigmoid function. Parameter γ in the channel-selection method was set to 0.5 in all experiments unless otherwise stated.

4) *Evaluation metrics*: The performance evaluation metrics include STOI [29], perceptual evaluation of speech quality (PESQ) [30], and signal to distortion ratio (SDR) [31]. STOI evaluates the objective speech intelligibility of time-domain signals. It has been shown empirically that STOI scores are well correlated with human speech intelligibility scores [5], [32]–[34]. PESQ is a test methodology for automated assessment of the speech quality as experienced by a listener of a telephony system. SDR is a metric similar to SNR for evaluating the quality of enhancement. The higher the value of an evaluation metric is, the better the performance is.

Because the distances between the speech source and the microphone arrays do not distribute uniformly in the rooms, we propose the *probabilistic average* and *probabilistic standard deviation* to evaluate the performance of a comparison method in a distance range of the rooms:

$$E_{[a,c]} = \frac{\int_a^c \text{perf}(x)p(x)dx}{\int_a^c p(x)dx} \quad (29)$$

$$\approx \frac{\sum_{i=a}^{c-b} \text{perf}(i+b) \int_i^{i+b} p(x)dx}{\sum_{i=a}^{c-b} \int_i^{i+b} p(x)dx} \quad (30)$$

$$S_{[a,c]} = \frac{\int_a^c |\text{perf}(x) - E_{[a,c]}| p(x)dx}{\int_a^c p(x)dx} \quad (31)$$

$$\approx \frac{\sum_{i=a}^{c-b} |\text{perf}(i+b) - E_{[a,c]}| \int_i^{i+b} p(x)dx}{\sum_{i=a}^{c-b} \int_i^{i+b} p(x)dx} \quad (32)$$

where $E_{[a,c]}$ and $S_{[a,c]}$ are the probabilistic average and probabilistic standard deviation respectively over a range of $[a, c]$ meters, $p(x)$ is the PDF at a distance x , and $\text{perf}(x)$ is the performance of the method at x which can be STOI, PESQ, SDR, etc. Because we evaluated the performance every 1 other meter, i.e. $b = 1$, we adopted the approximation equations (30) and (32) eventually.

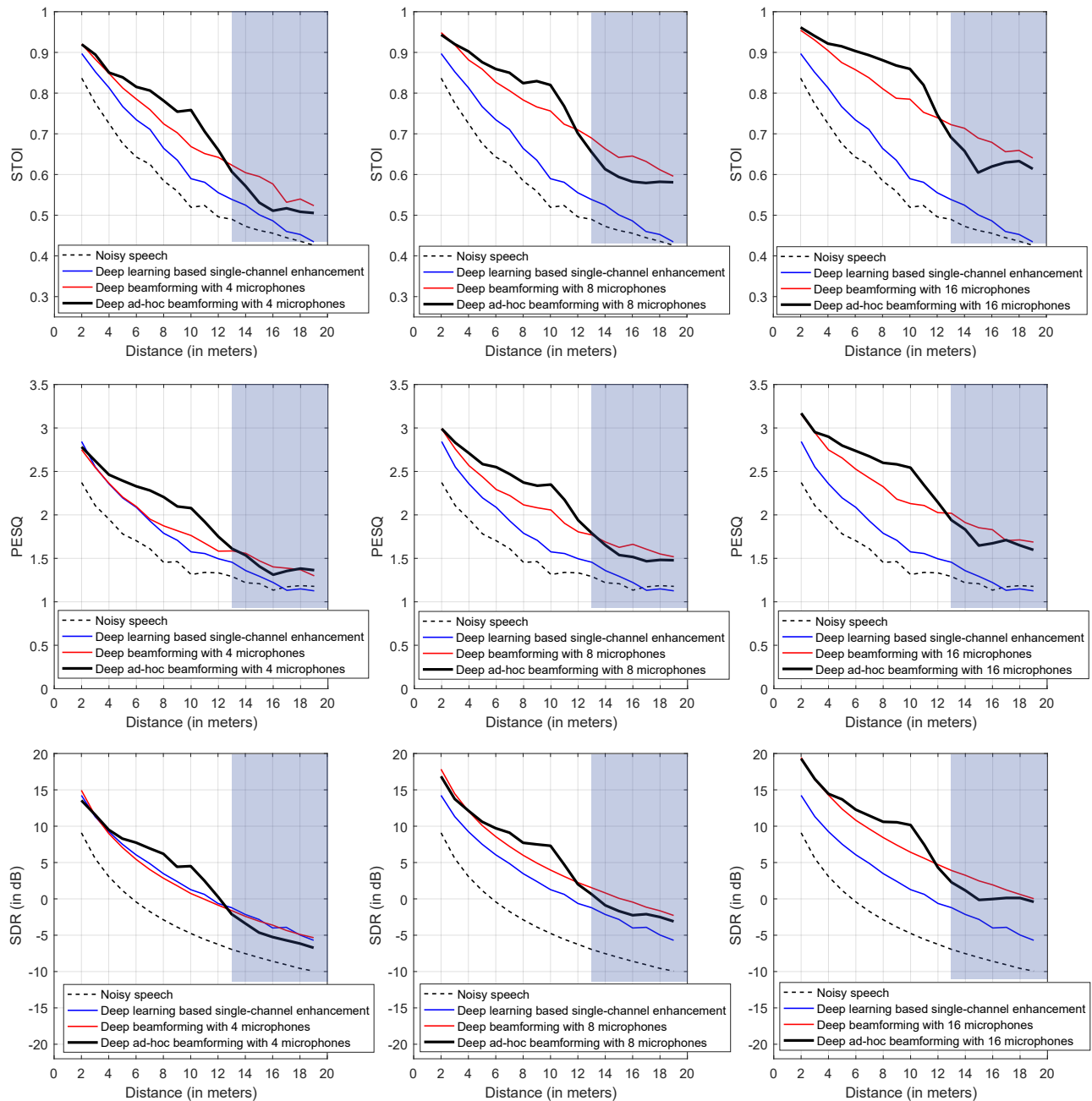


Fig. 7. Performance curves of the DNN-based nonlinear single-channel speech enhancement (DS), deep beamforming (DB), and deep ad-hoc beamforming (DAB) with respect to the distances between the speech source and the microphone arrays in the babble noise scenario. All DNN models were trained noise-dependently. The distances between the speech source and the DAB with 4, 8, and 16 microphones that fall into the shadow areas happens with probabilities of 2.83%, 1.12%, and 0.34%, respectively.

B. Main results

Figure 7 shows the comparison result of DS, DB, and DAB in the babble noise scenario. From the figure, we observe that DAB outperforms DS and DB in the distance range of $[1, 13)$ meters, while it sometimes behaves poorer than DB in the distance range of $[13, 20]$ meters. However, the ad-hoc microphone arrays seldom fall into $[13, 20]$ meters. Specifically, we find from Fig. 6 that the ad-hoc microphone arrays with 4, 8, and 16 microphones that fall into the range of $[13, 20]$ meters have probabilities of only 2.83%, 1.12%, and 0.34% respectively. We also observe that DAB behaves more

robust than DS and DB in the distance range of $[1, 10]$ meters, and the relative performance improvement over DS and DB reaches the maximum when the distance is around 10 meters; on the contrary, DAB seems behave less robust than DS and DB in the distance range of $(10, 20]$ meters. At last, we see that both DB and DAB benefits much from the increase of the microphone number.

To study the overall performance of DAB, we list the probabilistic average and probabilistic standard deviation performance of the comparison methods in the three noise scenarios in Tables II and III. From Table II where DB and DAB

TABLE II

PROBABILISTIC AVERAGE AND PROBABILISTIC STANDARD DEVIATION OF THE DS, DB, AND DAB WITH NOISE-DEPENDENT TRAINING, WHERE BOTH DB AND DAB CONSIST OF 4 MICROPHONES. THE NUMBERS IN BRACKETS ARE THE PROBABILISTIC STANDARD DEVIATIONS. THE TERM ‘‘PROBABILITY’’ DESCRIBES THE PROBABILITY OF THE DISTANCE THAT FALLS INTO A PREDEFINED RANGE. SEE (30) AND (32) FOR THE CALCULATION METHOD OF THE PROBABILISTIC AVERAGE AND PROBABILISTIC STANDARD DEVIATION.

Distance range		Babble			Factory			Volvo			Probability
		STOI	PESQ	SDR	STOI	PESQ	SDR	STOI	PESQ	SDR	
(0, 10]	Noisy	0.6535 (0.0766)	1.73 (0.25)	0.29 (3.49)	0.6395 (0.0814)	1.58 (0.26)	0.28 (3.49)	0.9160 (0.0204)	3.14 (0.24)	0.26 (3.50)	76.47%
	DS	0.7338 (0.0756)	2.09 (0.31)	6.44 (3.24)	0.7417 (0.0695)	2.06 (0.31)	7.77 (2.97)	0.9557 (0.0111)	3.78 (0.16)	22.20 (2.02)	76.47%
	DB	0.7838 (0.0636)	2.13 (0.27)	6.07 (3.57)	0.7772 (0.0700)	2.01 (0.27)	5.89 (3.58)	0.9339 (0.0213)	3.14 (0.23)	6.25 (3.49)	76.47%
	DAB	0.7975 (0.0269)	2.25 (0.10)	6.66 (1.28)	0.7978 (0.0297)	2.14 (0.11)	6.42 (1.10)	0.9129 (0.0115)	3.25 (0.06)	6.88 (1.03)	87.58%
(10, 20]	Noisy	0.4910 (0.0201)	1.28 (0.06)	-6.82 (0.94)	0.4775 (0.0225)	1.15 (0.09)	-6.84 (0.95)	0.8699 (0.0099)	2.67 (0.08)	-6.90 (0.95)	23.53%
	DS	0.5409 (0.0282)	1.43 (0.10)	-1.19 (1.24)	0.5646 (0.0332)	1.41 (0.10)	0.69 (1.13)	0.9292 (0.0069)	3.41 (0.08)	18.05 (0.61)	23.53%
	DB	0.6223 (0.0249)	1.57 (0.07)	-1.54 (1.11)	0.6038 (0.0210)	1.47 (0.09)	-1.71 (1.02)	0.8748 (0.0102)	2.61 (0.06)	-1.02 (0.96)	23.53%
	DAB	0.6660 (0.0388)	1.79 (0.13)	0.68 (1.79)	0.6529 (0.0356)	1.70 (0.11)	0.74 (1.48)	0.8451 (0.0186)	2.78 (0.14)	0.70 (1.33)	12.42%
(0, 20]	Noisy	0.6153 (0.0893)	1.62 (0.27)	-1.38 (3.88)	0.6013 (0.0897)	1.48 (0.27)	-1.39 (3.89)	0.9052 (0.0243)	3.03 (0.26)	-1.42 (3.90)	—
	DS	0.6884 (0.0988)	1.93 (0.36)	4.64 (3.89)	0.7000 (0.0869)	1.91 (0.35)	6.10 (3.55)	0.9495 (0.0134)	3.69 (0.19)	21.22 (2.25)	—
	DB	0.7458 (0.0819)	2.00 (0.30)	4.28 (4.05)	0.7364 (0.0863)	1.88 (0.30)	4.10 (4.05)	0.9200 (0.0278)	3.01 (0.26)	4.54 (3.95)	—
	DAB	0.7812 (0.0396)	2.20 (0.15)	5.92 (1.94)	0.7798 (0.0437)	2.08 (0.15)	5.71 (1.67)	0.9045 (0.0184)	3.19 (0.11)	6.11 (1.66)	—

TABLE III

PROBABILISTIC AVERAGE AND PROBABILISTIC STANDARD DEVIATION OF THE DS, DB, AND DAB WITH NOISE-DEPENDENT TRAINING, WHERE BOTH DB AND DAB CONSIST OF 16 MICROPHONES.

Distance range		Babble			Factory			Volvo			Probability
		STOI	PESQ	SDR	STOI	PESQ	SDR	STOI	PESQ	SDR	
(0, 10]	Noisy	0.6535 (0.0766)	1.73 (0.25)	0.29 (3.49)	0.6395 (0.0814)	1.58 (0.26)	0.28 (3.49)	0.9160 (0.0204)	3.14 (0.24)	0.26 (3.50)	76.47%
	DS	0.7338 (0.0756)	2.09 (0.31)	6.44 (3.24)	0.7417 (0.0695)	2.06 (0.31)	7.77 (2.97)	0.9557 (0.0111)	3.78 (0.16)	22.20 (2.02)	76.47%
	DB	0.8560 (0.0463)	2.54 (0.26)	11.39 (3.29)	0.8646 (0.0521)	2.49 (0.26)	11.82 (3.36)	0.9616 (0.0145)	3.50 (0.18)	12.59 (3.31)	76.47%
	DAB	0.8866 (0.0142)	2.65 (0.07)	11.31 (0.79)	0.8988 (0.0136)	2.58 (0.06)	11.53 (0.94)	0.9590 (0.0063)	3.67 (0.07)	12.07 (0.81)	92.91%
(10, 20]	Noisy	0.4910 (0.0201)	1.28 (0.06)	-6.82 (0.94)	0.4775 (0.0225)	1.15 (0.09)	-6.84 (0.95)	0.8699 (0.0099)	2.67 (0.08)	-6.90 (0.95)	23.53%
	DS	0.5409 (0.0282)	1.43 (0.10)	-1.19 (1.24)	0.5646 (0.0332)	1.41 (0.10)	0.69 (1.13)	0.9292 (0.0069)	3.41 (0.08)	18.05 (0.61)	23.53%
	DB	0.7242 (0.0225)	1.99 (0.09)	4.04 (1.14)	0.7211 (0.0296)	1.91 (0.10)	4.49 (1.06)	0.9263 (0.0083)	3.07 (0.07)	5.41 (0.96)	23.53%
	DAB	0.7963 (0.0338)	2.27 (0.10)	6.43 (1.43)	0.8101 (0.0340)	2.21 (0.12)	6.82 (1.21)	0.9187 (0.0105)	3.27 (0.12)	7.63 (1.08)	7.09%
(0, 20]	Noisy	0.6153 (0.0893)	1.62 (0.27)	-1.38 (3.88)	0.6013 (0.0897)	1.48 (0.27)	-1.39 (3.89)	0.9052 (0.0243)	3.03 (0.26)	-1.42 (3.90)	—
	DS	0.6884 (0.0988)	1.93 (0.36)	4.64 (3.89)	0.7000 (0.0869)	1.91 (0.35)	6.10 (3.55)	0.9495 (0.0134)	3.69 (0.19)	21.22 (2.25)	—
	DB	0.8250 (0.0630)	2.41 (0.30)	9.66 (3.79)	0.8309 (0.0688)	2.35 (0.31)	10.09 (3.85)	0.9533 (0.0174)	3.40 (0.22)	10.90 (3.82)	—
	DAB	0.8802 (0.0196)	2.62 (0.09)	10.96 (1.07)	0.8925 (0.0187)	2.55 (0.08)	11.2 (1.20)	0.9561 (0.0087)	3.64 (0.09)	11.76 (1.06)	—

consist of 4 microphones, we find that DAB outperforms the comparison methods in the babble and factory noise environments in terms of STOI and PESQ; it also outperforms DB in the volvo environment in terms of PESQ and SDR. We also see that DAB yields much smaller probabilistic standard deviations than the comparison methods in the distance ranges of (0, 10] and the entire (0, 20] meters; although the probabilistic standard deviations of DAB are slightly larger than the comparison methods in the range of (10, 20] meters, this situation happens with a probability of only 12.42%.

Comparing Table II with Table III where DB and DAB consist of 16 microphones, we find an important advantage of DAB: the improvement of DAB over DB tends to be enlarged when the number of the microphones is increased. We take the performance in the entire distance range (0, 20] as an example. The relative improvement of the probabilistic average of DAB over DB is increased from 13.93% to 31.54%, and meanwhile the relative reduction of the probabilistic standard deviation is improved from 51.65% to 68.89% in terms of STOI in the babble noise scenario, so as to other evaluation metrics and noise scenarios. Particularly, DAB outperforms the comparison methods in the volvo noise environment in terms

of STOI and PESQ, which is not the case when the number of the microphones is 4. Essentially, the above advantage comes from the increased probability density of the distributed microphones in the rooms, which makes more microphones have a high probability to be close to the speech source.

C. Analysis of the channel-reweighting algorithm

This subsection analyze the two components of the channel-reweighting algorithm respectively in the babble noise scenario when the microphone number of DAB is set to 16.

1) *On the channel-reweighting model:* This subsection analyze the input features, models, and output targets of the channel-reweighting model, respectively.

The channel-reweighting model takes the combination of the pooling features of the noisy speech and enhanced speech as its input. To verify that using the combined feature is a good choice, we compared the combined feature with its components. Figures 8 and 9 show the training loss and test results respectively of the channel-reweighting model with different features. From Fig. 8, we see that the combined feature achieves apparently lower training loss than its components. From Fig. 9, we see that the combined feature yields the best

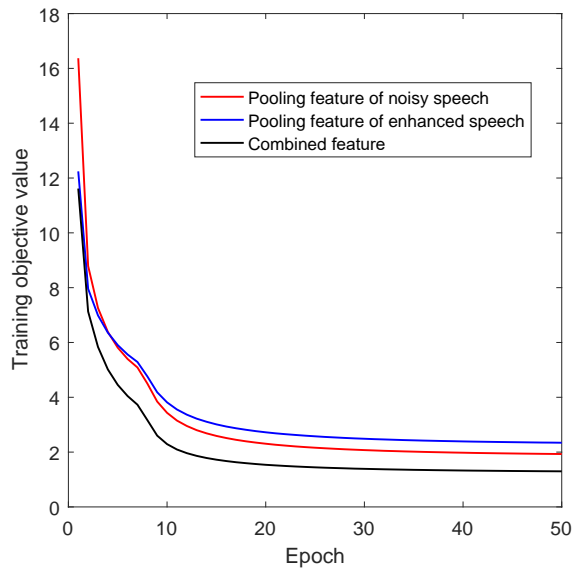


Fig. 8. Curves of the training loss of the channel-reweighting model with different input features.

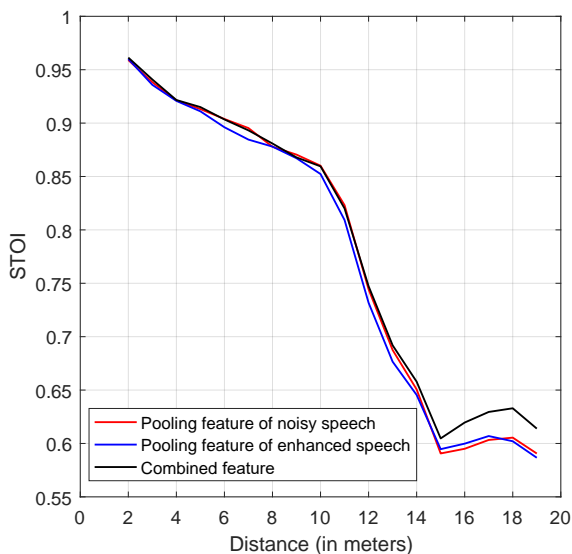


Fig. 9. STOI curves of the channel-reweighting model with different input features.

performance, while the pooling feature of the noisy speech yields similar performance with the combined feature in most cases.

The channel-reweighting model takes DNN as the regression model. To verify that DNN is a valid model, we compared it with linear regression. The normalized estimation error of the comparison methods, which is defined as $|p_{\text{opt}} - p|/p_{\text{opt}}$ with p_{opt} as the ground-truth, are shown in Fig. 10. From the figure, we see that the estimation error produced by DNN is 50% lower than that produced by linear regression. The STOI performance of the comparison methods in Fig. 11 shows that DNN produces a higher STOI curve than linear regression.

The channel-reweighting model in the previous experiments takes DAB-S2NR as the training target. To verify that DAB-S2NR is a plausible training target, we compared it with DAB-

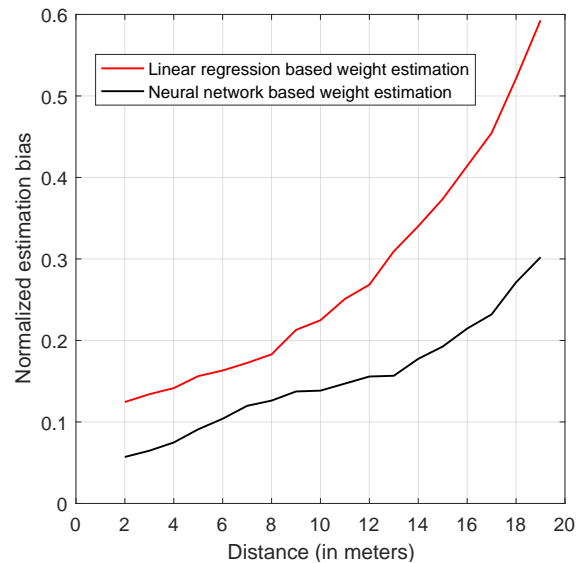


Fig. 10. Normalized estimation errors of the channel weights produced by neural networks and linear regression respectively. The normalized estimation error is defined as $|p_{\text{opt}} - p|/p_{\text{opt}}$ where p_{opt} is the ground-truth and p is the estimated weight.

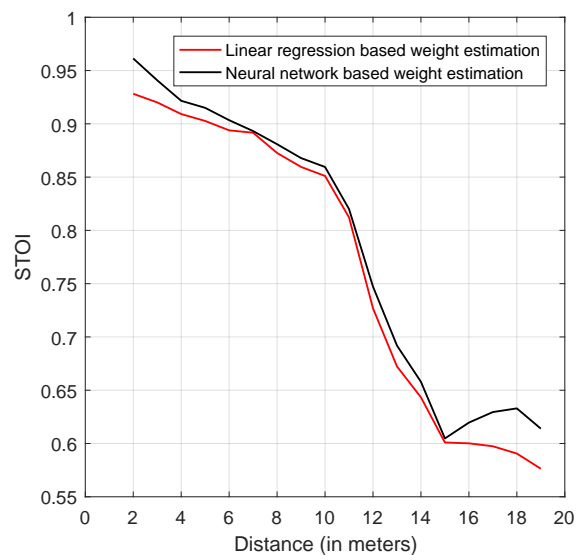


Fig. 11. STOI curves produced by neural networks and linear regression.

SNR. From the comparison result in Fig. 12, we observe the following two experimental phenomena. First, setting $\gamma = 0$ means that no channel-selection was conducted. In this case, DAB-S2NR is much worse than DAB-SNR, since the ground-truth of DAB-S2NR assigns much higher weights to the channels that are completely noisy than that of DAB-SNR. However, when we activated the channel-selection method by setting $\gamma = 0.5$, we observe that DAB-S2NR and DAB-SNR yields similar STOI curves. Hence, we can use either of them in practice.

2) *On the channel-selection method:* This subsection first studies the effect of parameter γ , and then compares DAB with its variants that adopt different channel-selection methods.

Parameter γ has a significant impact on the performance.

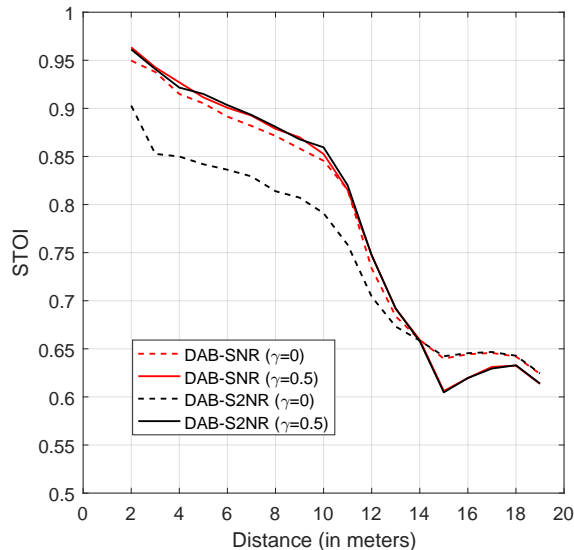


Fig. 12. STOI curves of the channel-reweighting model with DAB-SNR and DAB-S2NR as the training targets respectively.

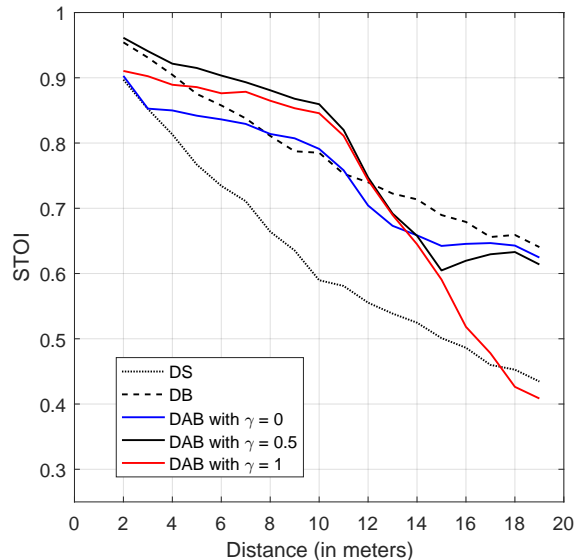


Fig. 13. STOI curves of the channel-reweighting algorithm with different γ . When $\gamma = 0$, only the channel with the largest weight is selected. When $\gamma = 1$, all channels are used. Setting $\gamma = 0.5$ is the default which disables only part of the channels.

Setting $\gamma = 0$ results in $\mathbf{b} = \mathbf{1}$ in (23), in other words, all channels are activated by DAB. When setting $\gamma = 1$, only the channel with the highest estimated weight, denoted as *the best channel*, is selected. Setting $0 < \gamma < 1$ compromises the above two extreme parameter settings, where we find that setting $\gamma = 0.5$ yields the optimal performance in general. An example is shown in Fig. 13. From the figure, we also find that the method of selecting the best channel is even better than that of activating all channels in most cases.

To further validate the channel-selection method, we compared it with its variants including (i) a method that does not use the channel-reweighting algorithm, i.e. $\mathbf{p} = \mathbf{1}$, (ii) a method that outputs the noisy speech from the best channel

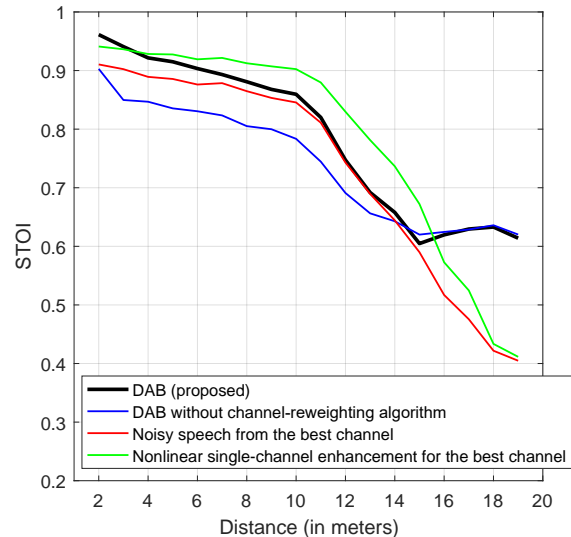


Fig. 14. STOI curves of the proposed DAB and its three variants. The first variant, named “DAB without channel-reweighting algorithm”, regards all channels of the ad-hoc microphone array as equally important. The second variant, named “noisy speech from the best channel”, takes the noisy speech received by the microphone that has the largest weight among the weights produced by the channel-reweighting model as the final output of DAB. The third variant, named “DS for the best channel of DAB”, enhances the single-channel noisy speech produced from the second variant of DAB by DS.

directly, and (iii) a method that uses a single-channel DNN to enhance the noisy speech received by the best channel. We name the above three variants as *variant 1*, *variant 2*, and *variant 3*, respectively for brevity. Figure 14 shows the STOI curves of the comparison methods. Table IV lists the probabilistic averages and probabilistic standard deviations of the comparison methods in the entire distance range. From the figure and the table, we see the following phenomena. First, the proposed channel-reweighting algorithm is effective compared to *variant 1*. For example, it improves the STOI score from 80.78% to 88.02%. Second, the proposed channel-selection method improves the STOI score from 86.25% made by *variant 2* to 88.02%.

Third, the proposed DAB is not as good as *variant 3* in general. A plausible explanation is that the enhancement ability of DAB relies on the number of the activated channels. When the number of the activated channels is large enough, DAB is in fact able to outperform *variant 3*. A direct proof for this claim can be observed in the distance ranges of $(0, 3]$ and $(15, 20]$, where the distributions of the microphones are more concentrated than those elsewhere. Hence, how to place the microphones and cluster them into groups when their number is limited is important. This topic is out of our discussion, we leave it as future work.

VI. EXPERIMENTS WITH NOISE-INDEPENDENT MODELS

The term *noise-independent* means that once trained, DAB can achieve reasonable performance in various noise scenarios, even though the noise scenarios are unseen from the training set. Training good noise-independent models is one of the ultimate goals of DAB in real-world applications and also one of the most difficult tasks that prohibit machine learning

TABLE IV
PERFORMANCE ANALYSIS OF THE PROPOSED DAB AND ITS THREE
VARIANTS. SEE FIG. 14 FOR THE DESCRIPTION OF THE TREE VARIANTS.

	Babble		
	STOI	PESQ	SDR
DAB (proposed)	0.8802 (0.0196)	2.62 (0.09)	10.96 (1.07)
DAB without channel-reweighting algorithm	0.8078 (0.0196)	2.43 (0.09)	4.91 (0.41)
Noisy speech from the best channel of DAB	0.8625 (0.0165)	2.46 (0.06)	10.65 (0.86)
DS for the best channel of DAB	0.9115 (0.0100)	2.98 (0.06)	15.30 (0.60)

methods from practical use. In this section, we evaluate the performance of DAB with noise-independent models in difficult and unseen test scenarios.

A. Experimental settings

The difference between the experimental settings here and that in Section V-A is mainly on the datasets. To synthesize the training data, we used TIMIT as the clean speech source, and used a large-scale sound effect library³ as the noise corpus [35], [36] which contains over 20,000 sound effects. We randomly partitioned the noise corpus to two parts. The first part was used to synthesize 100,000 noisy training utterances for DNN1. The second part was used to synthesize 1,000,000 noisy training utterances for DNN2. Each training utterance was synthesized in the same way as that in Section V-A except that the SNR at the origin was randomly generated from a range of [5, 25] dB. To synthesize the test data, we followed the same way as that in Section V-A except that the SNRs at the origin contain three levels: 10, 15, and 20 dB. Besides, we set DNN2 to two hidden layers with 1024 units per layer.

B. Results

Tables V and VI list the comparison results. Comparing Tables V and VI with Tables II and III respectively, we find that, when the SNRs at the origin were both set to 15 dB, the performance of all comparison methods with the noise-independent training is only slightly worse than the performance of their counterparts with the noise-dependent training, which indicates the good generalization ability of the comparison methods to unseen test scenarios. Moreover, we find that the advantages of DAB over DS and DB are consistent across the SNR levels and across both the noise-independent models and the noise-dependent models.

VII. CONCLUSIONS

In this paper, we have proposed deep ad-hoc beamforming, which is to our knowledge the first deep beamforming method for ad-hoc microphone arrays. Compared to DB, DAB has two novel aspects. First, DAB employs an ad-hoc microphone array to pick up speech signals, which has a potential to enhance the speech signals with equally high quality in a range where the array covers. It may also significantly reduce the high propagation cost of speech signals in the air by physically placing some microphones close to the speech source in probability. Second, DAB employs a channel-reweighting

algorithm to reweight the estimated speech signals with a sparsity constraint before conducting the MVDR beamforming, where the weights produced by DNN2 are an estimation of DAB-S2NR or DAB-SNR, and the sparsity constraint aims to filter out the microphones with relatively low weights. We have conducted an extensive experiment in the scenario where the location of the speech source is far-field, random, and blind to the microphones. Experimental results with both the noise-dependent training and noise-independent training demonstrate that DAB outperforms DS and DB by a large margin. Moreover, the probability standard deviation of DAB is also much smaller than those of DS and DB, which indicates the strong stability of DAB.

REFERENCES

- [1] D. Wang and J. Chen, "Supervised speech separation based on deep learning: An overview," *IEEE/ACM Transactions on Audio, Speech, and Language Processing*, 2018.
- [2] Y. Wang and D. L. Wang, "Towards scaling up classification-based speech separation," *IEEE Trans. Audio, Speech, Lang. Process.*, vol. 21, no. 7, pp. 1381–1390, 2013.
- [3] Y. Xu, J. Du, L.-R. Dai, and C.-H. Lee, "A regression approach to speech enhancement based on deep neural networks," *IEEE/ACM Trans. Audio, Speech, Lang. Process.*, vol. 23, no. 1, pp. 7–19, 2015.
- [4] Y. Jiang, D. Wang, R. Liu, and Z. Feng, "Binaural classification for reverberant speech segregation using deep neural networks," *IEEE/ACM Transactions on Audio, Speech and Language Processing (TASLP)*, vol. 22, no. 12, pp. 2112–2121, 2014.
- [5] Y. Wang, A. Narayanan, and D. L. Wang, "On training targets for supervised speech separation," *IEEE/ACM Trans. Audio, Speech, Lang. Process.*, vol. 22, no. 12, pp. 1849–1858, 2014.
- [6] J. Heymann, L. Drude, and R. Haeb-Umbach, "Neural network based spectral mask estimation for acoustic beamforming," in *Acoustics, Speech and Signal Processing (ICASSP), 2016 IEEE International Conference on*. IEEE, 2016, pp. 196–200.
- [7] T. Higuchi, N. Ito, T. Yoshioka, and T. Nakatani, "Robust mvdr beamforming using time-frequency masks for online/offline asr in noise," in *Acoustics, Speech and Signal Processing (ICASSP), 2016 IEEE International Conference on*. IEEE, 2016, pp. 5210–5214.
- [8] H. Erdogan, J. R. Hershey, S. Watanabe, M. I. Mandel, and J. Le Roux, "Improved mvdr beamforming using single-channel mask prediction networks," in *Interspeech*, 2016, pp. 1981–1985.
- [9] B. Li, T. N. Sainath, R. J. Weiss, K. W. Wilson, and M. Bacchiani, "Neural network adaptive beamforming for robust multichannel speech recognition," in *INTERSPEECH*, 2016, pp. 1976–1980.
- [10] L. Pfeifenberger, M. Zöhrer, and F. Pernkopf, "Dnn-based speech mask estimation for eigenvector beamforming," in *Acoustics, Speech and Signal Processing (ICASSP), 2017 IEEE International Conference on*. IEEE, 2017, pp. 66–70.
- [11] S. Bu, Y. Zhao, M.-Y. Hwang, and S. Sun, "A probability weighted beamformer for noise robust asr," to appear in *Interspeech*, 2018.
- [12] Z.-Q. Wang and D. Wang, "On spatial features for supervised speech separation and its application to beamforming and robust asr," in *2018 IEEE International Conference on Acoustics, Speech and Signal Processing (ICASSP)*. IEEE, 2018, pp. 5709–5713.
- [13] Z.-Q. Wang and D. Wang, "All-neural multichannel speech enhancement," to appear in *Interspeech*, 2018.
- [14] X. Xiao, S. Zhao, D. L. Jones, E. S. Chng, and H. Li, "On time-frequency mask estimation for mvdr beamforming with application in robust speech recognition," in *Acoustics, Speech and Signal Processing (ICASSP), 2017 IEEE International Conference on*. IEEE, 2017, pp. 3246–3250.
- [15] Y.-H. Tu, J. Du, L. Sun, and C.-H. Lee, "Lstm-based iterative mask estimation and post-processing for multi-channel speech enhancement," in *Asia-Pacific Signal and Information Processing Association Annual Summit and Conference (APSIPA ASC), 2017*. IEEE, 2017, pp. 488–491.
- [16] T. Higuchi, K. Kinoshita, N. Ito, S. Karita, and T. Nakatani, "Frame-by-frame closed-form update for mask-based adaptive mvdr beamforming," in *2018 IEEE International Conference on Acoustics, Speech and Signal Processing (ICASSP)*. IEEE, 2018, pp. 531–535.

TABLE V

PROBABILISTIC AVERAGE AND PROBABILISTIC STANDARD DEVIATION OF THE DS, DB, AND DAB WITH NOISE-INDEPENDENT TRAINING, WHERE BOTH DB AND DAB CONSIST OF 4 MICROPHONES. THE PHRASE ‘‘SNR AT THE ORIGIN’’ DENOTES THE SNR LEVEL AT THE LOCATION OF 1 METER AWAY FROM THE SPEECH SOURCE. THE REPORTED PERFORMANCE IS THE AVERAGE ONE OVER THE DISTANCE RANGE OF THE ENTIRE [1, 20] METERS.

SNR at the origin		Babble			Factory			Volvo		
		STOI	PESQ	SDR	STOI	PESQ	SDR	STOI	PESQ	SDR
10dB	Noisy	0.5100 (0.0826)	1.35 (0.20)	-6.16 (3.75)	0.4930 (0.0855)	1.20 (0.22)	-6.18 (3.76)	0.8711 (0.0295)	2.70 (0.27)	-6.25 (3.79)
	DS	0.5467 (0.1071)	1.54 (0.32)	-1.14 (4.69)	0.5568 (0.1070)	1.53 (0.34)	1.44 (4.03)	0.9103 (0.0229)	3.24 (0.24)	16.23 (2.06)
	DB	0.6215 (0.0987)	1.64 (0.28)	-1.33 (4.38)	0.6116 (0.1003)	1.49 (0.30)	-1.42 (4.23)	0.8779 (0.0358)	2.66 (0.28)	-0.13 (3.86)
	DAB	0.6837 (0.0474)	1.85 (0.14)	1.28 (2.15)	0.6728 (0.0521)	1.71 (0.15)	1.13 (2.02)	0.8702 (0.0220)	2.90 (0.12)	1.93 (1.78)
15dB	Noisy	0.6154 (0.0906)	1.63 (0.26)	-1.38 (3.88)	0.5995 (0.0897)	1.48 (0.26)	-1.39 (3.88)	0.9058 (0.0249)	3.04 (0.27)	-1.42 (3.90)
	DS	0.6776 (0.0980)	1.95 (0.33)	4.55 (3.80)	0.6826 (0.0905)	1.95 (0.34)	6.34 (3.13)	0.9354 (0.0157)	3.53 (0.21)	18.79 (1.86)
	DB	0.7438 (0.0804)	1.98 (0.30)	4.20 (4.07)	0.7326 (0.0870)	1.88 (0.30)	3.95 (4.09)	0.9202 (0.0247)	2.99 (0.23)	4.77 (3.76)
	DAB	0.7769 (0.0414)	2.17 (0.15)	5.53 (1.88)	0.7798 (0.0403)	2.09 (0.14)	5.83 (1.58)	0.9016 (0.0181)	3.15 (0.13)	6.07 (1.72)
20dB	Noisy	0.7254 (0.0795)	1.96 (0.29)	3.54 (3.92)	0.7141 (0.0870)	1.83 (0.29)	3.54 (3.93)	0.9344 (0.0194)	3.38 (0.26)	3.52 (3.93)
	DS	0.7914 (0.0686)	2.36 (0.30)	9.13 (3.12)	0.7923 (0.0683)	2.37 (0.30)	10.21 (2.81)	0.9536 (0.0110)	3.79 (0.16)	21.10 (1.61)
	DB	0.8358 (0.0565)	2.36 (0.27)	9.33 (3.87)	0.8373 (0.0647)	2.26 (0.30)	9.13 (3.95)	0.9499 (0.0162)	3.26 (0.18)	9.50 (3.49)
	DAB	0.8491 (0.0306)	2.50 (0.12)	9.28 (1.42)	0.8574 (0.0286)	2.44 (0.14)	9.27 (1.25)	0.9213 (0.0167)	3.31 (0.12)	9.41 (1.51)

TABLE VI

PROBABILISTIC AVERAGE AND PROBABILISTIC STANDARD DEVIATION OF THE DS, DB, AND DAB WITH NOISE-INDEPENDENT TRAINING, WHERE BOTH DB AND DAB CONSIST OF 16 MICROPHONES.

SNR at the origin		Babble			Factory			Volvo		
		STOI	PESQ	SDR	STOI	PESQ	SDR	STOI	PESQ	SDR
10dB	Noisy	0.5100 (0.0826)	1.35 (0.20)	-6.16 (3.75)	0.4930 (0.0855)	1.20 (0.22)	-6.18 (3.76)	0.8711 (0.0295)	2.70 (0.27)	-6.25 (3.79)
	DS	0.5467 (0.1071)	1.54 (0.32)	-1.14 (4.69)	0.5568 (0.1070)	1.53 (0.34)	1.44 (4.03)	0.9103 (0.0229)	3.24 (0.24)	16.23 (2.06)
	DB	0.7058 (0.0934)	1.96 (0.33)	4.04 (4.29)	0.6842 (0.1078)	1.86 (0.36)	4.12 (4.48)	0.9217 (0.0254)	3.03 (0.21)	6.17 (3.71)
	DAB	0.8027 (0.0254)	2.28 (0.10)	7.09 (1.26)	0.8046 (0.0276)	2.18 (0.09)	7.35 (1.14)	0.9350 (0.0076)	3.35 (0.07)	8.36 (1.07)
15dB	Noisy	0.6154 (0.0906)	1.63 (0.26)	-1.38 (3.88)	0.5995 (0.0897)	1.48 (0.26)	-1.39 (3.88)	0.9058 (0.0249)	3.04 (0.27)	-1.42 (3.90)
	DS	0.6776 (0.0980)	1.95 (0.33)	4.55 (3.80)	0.6826 (0.0905)	1.95 (0.34)	6.34 (3.13)	0.9354 (0.0157)	3.53 (0.21)	18.79 (1.86)
	DB	0.8153 (0.0661)	2.37 (0.29)	9.36 (3.78)	0.8108 (0.0795)	2.29 (0.31)	9.67 (3.96)	0.9485 (0.0157)	3.26 (0.14)	10.62 (3.25)
	DAB	0.8759 (0.0215)	2.60 (0.08)	10.74 (1.19)	0.8911 (0.0187)	2.56 (0.08)	11.02 (1.04)	0.9514 (0.0068)	3.56 (0.08)	11.79 (1.11)
20dB	Noisy	0.7254 (0.0795)	1.96 (0.29)	3.54 (3.92)	0.7141 (0.0870)	1.83 (0.29)	3.54 (3.93)	0.9344 (0.0194)	3.38 (0.26)	3.52 (3.93)
	DS	0.7914 (0.0686)	2.36 (0.30)	9.13 (3.12)	0.7923 (0.0683)	2.37 (0.30)	10.21 (2.81)	0.9536 (0.0110)	3.79 (0.16)	21.10 (1.61)
	DB	0.8905 (0.0427)	2.72 (0.24)	14.03 (3.24)	0.9014 (0.0465)	2.67 (0.26)	14.57 (3.47)	0.9647 (0.0080)	3.39 (0.08)	14.31 (2.22)
	DAB	0.9260 (0.0149)	2.92 (0.10)	13.80 (1.09)	0.9323 (0.0130)	2.87 (0.08)	13.29 (1.12)	0.9620 (0.0056)	3.63 (0.06)	14.05 (0.61)

- [17] Y. Zhou and Y. Qian, ‘‘Robust mask estimation by integrating neural network-based and clustering-based approaches for adaptive acoustic beamforming,’’ in *Int Conf on Acoustics, Speech, and Signal Processing, in press. Google Scholar*, 2018.
- [18] T. Nakatani, N. Ito, T. Higuchi, S. Araki, and K. Kinoshita, ‘‘Integrating dnn-based and spatial clustering-based mask estimation for robust mvdr beamforming,’’ in *Acoustics, Speech and Signal Processing (ICASSP), 2017 IEEE International Conference on*. IEEE, 2017, pp. 286–290.
- [19] X. Zhang, Z.-Q. Wang, and D. Wang, ‘‘A speech enhancement algorithm by iterating single-and multi-microphone processing and its application to robust asr,’’ in *Acoustics, Speech and Signal Processing (ICASSP), 2017 IEEE International Conference on*. IEEE, 2017, pp. 276–280.
- [20] R. Heusdens, G. Zhang, R. C. Hendriks, Y. Zeng, and W. B. Kleijn, ‘‘Distributed mvdr beamforming for (wireless) microphone networks using message passing,’’ in *Acoustic Signal Enhancement; Proceedings of IWAENC 2012; International Workshop on*. VDE, 2012, pp. 1–4.
- [21] Y. Zeng and R. C. Hendriks, ‘‘Distributed delay and sum beamformer for speech enhancement via randomized gossip,’’ *IEEE/ACM Transactions on Audio, Speech, and Language Processing*, vol. 22, no. 1, pp. 260–273, 2014.
- [22] M. O’Connor, W. B. Kleijn, and T. Abhayapala, ‘‘Distributed sparse mvdr beamforming using the bi-alternating direction method of multipliers,’’ in *Acoustics, Speech and Signal Processing (ICASSP), 2016 IEEE International Conference on*. IEEE, 2016, pp. 106–110.
- [23] M. O’Connor and W. B. Kleijn, ‘‘Diffusion-based distributed mvdr beamformer,’’ in *Acoustics, Speech and Signal Processing (ICASSP), 2014 IEEE International Conference on*. IEEE, 2014, pp. 810–814.
- [24] V. M. Tavakoli, J. R. Jensen, M. G. Christensen, and J. Benesty, ‘‘A framework for speech enhancement with ad hoc microphone arrays,’’ *IEEE/ACM Transactions on Audio, Speech and Language Processing (TASLP)*, vol. 24, no. 6, pp. 1038–1051, 2016.
- [25] S. Jayaprakasam, S. K. A. Rahim, and C. Y. Leow, ‘‘Distributed and collaborative beamforming in wireless sensor networks: Classifications, trends, and research directions,’’ *IEEE Communications Surveys & Tutorials*, vol. 19, no. 4, pp. 2092–2116, 2017.
- [26] V. M. Tavakoli, J. R. Jensen, R. Heusdens, J. Benesty, and M. G. Christensen, ‘‘Distributed max-sinr speech enhancement with ad hoc microphone arrays,’’ in *Acoustics, Speech and Signal Processing (ICASSP), 2017 IEEE International Conference on*. IEEE, 2017, pp. 151–155.
- [27] J. Zhang, S. P. Chepuri, R. C. Hendriks, and R. Heusdens, ‘‘Microphone subset selection for mvdr beamformer based noise reduction,’’ *IEEE/ACM Transactions on Audio, Speech, and Language Processing*, vol. 26, no. 3, pp. 550–563, 2018.
- [28] A. I. Koutrouvelis, T. W. Sherson, R. Heusdens, and R. C. Hendriks, ‘‘A low-cost robust distributed linearly constrained beamformer for wireless acoustic sensor networks with arbitrary topology,’’ *IEEE/ACM Transactions on Audio, Speech and Language Processing (TASLP)*, vol. 26, no. 8, pp. 1434–1448, 2018.
- [29] C. H. Taal, R. C. Hendriks, R. Heusdens, and J. Jensen, ‘‘An algorithm for intelligibility prediction of time-frequency weighted noisy speech,’’ *IEEE Trans. Audio, Speech, Lang. Process.*, vol. 19, no. 7, pp. 2125–2136, 2011.
- [30] A. W. Rix, J. G. Beerends, M. P. Hollier, and A. P. Hekstra, ‘‘Perceptual evaluation of speech quality (pesq)-a new method for speech quality assessment of telephone networks and codecs,’’ in *Proc. IEEE Int. Conf. Acoust., Speech, Signal Process.*, 2001, pp. 749–752.
- [31] E. Vincent, R. Gribonval, and C. F evotte, ‘‘Performance measurement in blind audio source separation,’’ *IEEE Trans. Audio, Speech, Lang.*

- Process.*, vol. 14, no. 4, pp. 1462–1469, 2006.
- [32] J. Du, Y. Tu, Y. Xu, L. Dai, and C.-H. Lee, “Speech separation of a target speaker based on deep neural networks,” in *Proc. IEEE Int. Conf. Signal Process.*, 2014, pp. 473–477.
- [33] P.-S. Huang, M. Kim, M. Hasegawa-Johnson, and P. Smaragdis, “Joint optimization of masks and deep recurrent neural networks for monaural source separation,” *IEEE/ACM Trans. Audio, Speech, Lang. Process.*, vol. 23, no. 12, pp. 2136–2147, 2015.
- [34] X.-L. Zhang and D. Wang, “A deep ensemble learning method for monaural speech separation,” *IEEE/ACM Transactions on Audio, Speech and Language Processing (TASLP)*, vol. 24, no. 5, pp. 967–977, 2016.
- [35] J. Chen, Y. Wang, S. Yoho, D. Wang, and E. Healy, “Large-scale training to increase speech intelligibility for hearing-impaired listeners in novel noises,” *Journal of the Acoustical Society of America*, vol. 139, no. 5, pp. 2604–2612, 2016.
- [36] X.-L. Zhang and D. Wang, “Boosting contextual information for deep neural network based voice activity detection,” *IEEE/ACM Transactions on Audio, Speech, and Language Processing*, vol. 24, no. 2, pp. 252–264, 2016.